Mott Insulating Ground State and its Proximity to Spin-Orbit Insulators in Na_2IrO_3

Hosub Jin,[1] Heungsik Kim,[1] Hogyun Jeong,[2] Choong H. Kim,[1] and Jaejun Yu[1,*]

[1]*Department of Physics and Astronomy, CSCMR, Center for Theoretical Physics, Seoul National University, Seoul 151-747, Korea*
[2]*Computational Science and Technology Interdisciplinary Program, Seoul National University, Seoul 151-747, Korea*

(Dated: July 4, 2009)

We present an anti-ferromagnetically ordered ground state of Na_2IrO_3 based on density-functional-theory calculations including both spin-orbit coupling and on-site Coulomb interaction U. We show that the splitting of e'_g doublet states by the strong spin-orbit coupling is mainly responsible for the intriguing nature of its insulating gap and magnetic ground state. Due to its proximity to the spin-orbit insulator phase, the magnetic ordering as obtained with finite U is found to exhibit a strong in-plane anisotropy. The phase diagram of Na_2IrO_3 suggests a possible interplay between spin-orbit insulator and Mott anti-ferromagnetic insulator phases.

PACS numbers: 71.70.Ej, 75.30.Kz, 71.20.-b, 75.30.Gw

arXiv:0907.0743v1 [cond-mat.str-el] 4 Jul 2009

Recently, the role of spin-orbit coupling (SOC) has attracted great attention in many fields of condensed matter physics. In multiferroic materials, for example, SOC combined with a large electron-lattice interaction has been suggested to be responsible for the multiferroic behavior which exhibit both non-collinear magnetic ordering and lattice polarization[1,2]. SOC is also indispensable to anomalous Hall and spin Hall effects where Hall and spin Hall currents are generated by an external electric field, respectively[3,4,5]. In particular, the quantum spin Hall effect has led to the notion of topological insulators, new states of quantum matter[6,7]. While they have bulk energy gaps generated by the SOC, topological insulators are characterized by the presence of gapless surface states which are protected by time-reversal symmetry[8].

Another manifestation of strong SOC combined with on-site Coulomb interactions is the $j_{\rm eff}$=1/2 Mott insulator discovered in Sr_2IrO_4, one of the 5d transition-metal oxides[9,10]. The novel spin-orbit integrated state with $j_{\rm eff}$=1/2 arises from the combined action of both strong SOC and intermediate on-site Coulomb interactions within the Ir 5d t_{2g} manifold. In addition, there has been a theoretical proposal on the room temperature quantum spin Hall effect in Na_2IrO_3 based on the $j_{\rm eff}$=1/2 physics[11], where the honeycomb lattice consisting of edge-shared IrO_6 octahedra in each Ir-O layer was considered to be an ideal realization of the Kane-Mele model, where hopping integrals between the $j_{\rm eff}$=1/2 states at the Fermi level was assumed to be an essential ingredient for the quantum spin Hall effect[8,12]. Since the crystal structure and local environment of Ir atoms in Na_2IrO_3 are different from those of Sr_2IrO_4, however, it is necessary to clarify the electronic and magnetic structures of the Ir 5d manifold in this Na_2IrO_3 compound with hexagonal lattice.

In this paper, we present novel electronic structure and magnetic properties of Na_2IrO_3 by carrying out density-functional-theory (DFT) calculations including both SOC $\lambda_{\rm SO}$ and on-site Coulomb interaction. We observe that a new form of spin-orbit coupled states emerges from the e'_g doublet states near the Fermi level ($E_{\rm F}$) and determines the intriguing nature of its insulating gap. With an effective on-site Coulomb interaction parameter $U = 2.0$ eV, the ground state of Na_2IrO_3 is found to be an antiferromagnetic (AFM) insulator with the ordered moments lying down within the honeycomb lattice of Ir atoms. The large splitting of the e'_g doublet by the strong SOC is related to the strong in-plane anisotropy of magnetic ordering. Considering the role of SOC, we propose a phase diagram in the $\lambda_{\rm SO}$–U parameter space which features a phase boundary between AFM Mott insulators and SO insulators. By estimating the exchange couplings between neighboring Ir atoms, we suggest a possible frustration of magnetic ordering in its ground state, which is consistent with a recent experiment[13].

In order to examine the effects of both SOC and on-site Coulomb interaction on the electronic structure of Na_2IrO_3, it is necessary to treat both SOC and U on an equal footing in the description of Ir 5d states. To identify the role of each contribution as well as the interplay between them, we carried out DFT calculations within the local-density approximation (LDA), LDA including SOC (LDA+SO), and LDA+U including SOC (LDA+U+SO) respectively. For the calculations, we used the DFT code, OpenMX[14], based on the linear-combination-of-pseudo-atomic-orbitals method[15], where both the LDA+U method[16] and the SOC contribution were included via a relativistic j-dependent pseudo-potential scheme in the non-collinear DFT formalism. Double valence and single polarization orbitals were used as basis sets, which were generated by a confinement potential scheme with cutoff radii of 7.0, 7.0 and 5.0 a.u. for Na, Ir, and O atoms respectively. We used a (14×14×14) **k**-point grid for the k-space integration.

Up to our knowledge there is no crystal structure data for Na_2IrO_3 published yet. Thanks to the preliminary information provided by Takagi[13], we were able to construct a minimal unit-cell containing two formula units based on the hexagonal structure of Na_2RuO_3[17], a sibling compound of Na_2IrO_3. The crystal structure of Na_2IrO_3 can be viewed as an alternate stacking of $(Ir_{2/3}Na_{1/3})O_2$ and Na layers. Edge-shared IrO_6 octahedra form a honeycomb lattice of Ir atoms. Na atoms are placed at the center of each hexagon. Upper and lower triangle oxygens are rotated by 3.5° to shorten the Ir-O distance. The positions of atoms in the unit cell were determined through the full structural optimization by the LDA calculations with 0.5×10^{-3} Hatree/Å of force criterion. There is a possible stacking disorder in the types of the Na-layers relative to the $(Ir_{2/3}Na_{1/3})O_2$ layers. We have checked the effect of different stacking sequences and observed a negligible change in the energy dispersions. Since the basic electronic

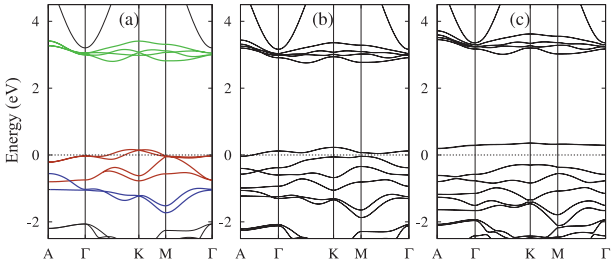

FIG. 1: (Color online) Electronic band structures of Na_2IrO_3 within (a) LDA, (b) LDA+SO, and (c) LDA+U+SO schemes. Green, red, and blue colored energy dispersions in (a) are indicating e_g, e'_g, and a_{1g} bands respectively, induced by the largest cubic and the next largest trigonal crystal fields.

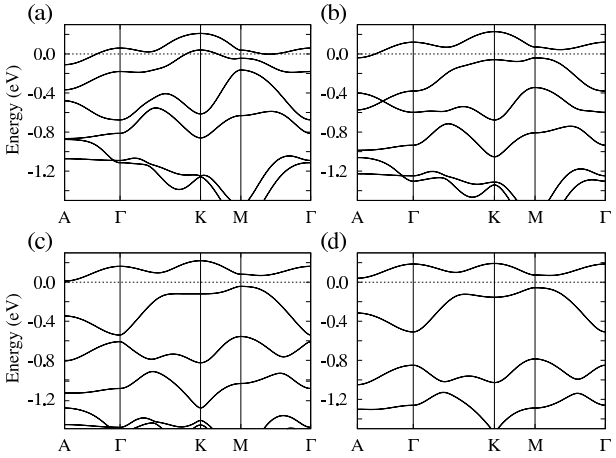

FIG. 2: Electronic band structures from LDA+SO calculations with the scaling factors of SOC strength λ_{SO}/λ_0 are (a) 0.5, (b) 1.0, (c) 1.5, and (d) 2.0, where λ_0 is the SOI magnitude of a real Ir atom. Gap opens when λ_{SO}/λ_0 is increasing from 1.0 to 1.5.

structure is dominated by the in-plane Ir-O hybridization and remains intact regardless of the stacking sequence, we will focus on the electronic structure without structural disorder hereafter.

We investigated the electronic and magnetic structures of Na_2IrO_3 by performing LDA, LDA+SO, and LDA+U+SO calculations. Calculated electronic band structure near E_F are shown in Fig. 1. The LDA band structure in Fig. 1(a) features the Ir 5d bands of e_g and t_{2g} components separated by a large cubic crystal field $\Delta_{\text{cubic}} \sim 4$ eV. While narrow e_g bands are located at 3 eV above E_F, the top of t_{2g} bands are pinned at E_F and spread out to -2.0 eV below E_F. Due to the extended nature of Ir 5d orbitals, there are large contributions to the band structure from both the indirect hopping via the Ir 5d-O 2p hybridization and the direct hopping between the neighboring Ir 5d orbitals. From the tight-binding analysis[18], even the next-nearest-neighbor hopping terms through oxygen and sodium atoms make significant contributions to the LDA band structure.

The trigonal crystal field (Δ_{trigonal}) splits the t_{2g} bands into a_{1g} and e'_g states. In addition, there is a strong hybridization between neighboring Ir 5d orbitals which gives rise to the bonding and anti-bonding of e'_g orbitals. The bonding and anti-bonding doublet states consist of e'_g orbital pairs of two Ir atoms per unit cell. At the Γ point of the LDA band structure, the e'_g anti-bonding states, to be called by e_{AB}, are close to E_F while the e'_g bonding states, to be called by e_B, are at about -0.8 eV. The a_{1g} bands located at -1 eV have a negligible effect of the hybridization between neighboring Ir atoms but show a relatively large c-axis dispersion, which may be derived from the character of a_{1g} orbitals pointing toward the Na atoms in the next layers. Here it is noted that the appearance of the e_{AB} doublet at E_F in the LDA band structure of Na_2IrO_3 is in contrast to the presence of almost degenerate t_{2g} state in Sr_2IrO_4 which serves as a basis for the j_{eff}=1/2 state when SOC is introduced[9].

In the LDA band structure, the doubly degenerate e_{AB} states form a narrow band and cross E_F. The introduction of SOC breaks the degeneracy of e_{AB} by preserving the time-reversal symmetry so that the e_{AB} bands split off over the whole Brillouin zone (BZ) as shown in Fig. 1(b). Despite the split of e_{AB} bands, the LDA+SO band structure is still metallic with a small electron pocket at the A point and hole pockets off the $k_c = 0$ plane near M. From the tight-binding analysis of the Na_2IrO_3 band structure[18], we obtained $\Delta_{\text{trigonal}} \sim 0.6$ eV, which is larger than the SOC parameter $\lambda_{SO} \sim 0.4$ eV[9,19]. Thus the band structure of Na_2IrO_3 near E_F is characterized by the bonding e_B and anti-bonding e_{AB} states with $\Delta_{\text{cubic}} > \Delta_{\text{trigonal}} > \lambda_{SO}$. Since $\Delta_{\text{trigonal}} > \lambda_{SO}$, however, the e_{AB} character of the bands are maintained. Contrary to the layered perovskite Sr_2IrO_4 system, where the SOC entangles almost degenerate t_{2g} orbitals with spin states and produces the spin-orbit integrated j_{eff}=1/2, the strong trigonal field in Na_2IrO_3 suppresses the mixing of a_{1g} and e'_g states. Instead, the SOC acting on the e'_g subspace plays a role of effective Zeeman coupling, the details of which will be discussed later. The presence of the effective Zeeman coupling is manifested in the parallel splitting of e_{AB} and e_B bands.

Similarly to the case of Sr_2IrO_4, both the on-site Coulomb interaction and the SOC are expected to be important in the description of Ir 5d states. The LDA+U+SO band structure shown in Fig. 1(c) was calculated with an effective $U = 2.0$ eV, which was found to be consistent with angle-resolved photoemission and optical spectroscopy experiments[9]. As a result of the combined action of both on-site Coulomb interaction and SOC, a small band gap arises between the SO-split e_{AB} bands. Two e_{AB} bands form valence and conduction bands with nearly the same dispersion above and below E_F, respectively. Contrary to the non-magnetic metallic solution of the LDA and LDA+SO calculations, the LDA+U+SO solution predicts an AFM ordering with local magnetic moments lying within the ab plane. The magnitude of total moment is 0.47 μ_B per each Ir atom, which is decomposed into the spin moment of 0.12 μ_B and the orbital moment of 0.35 μ_B.

Despite that the importance of both U and λ_{SO}, the nature of the insulating ground state of Na_2IrO_3 is quite distinct from that of Sr_2IrO_4. In Sr_2IrO_4, the j_{eff}=1/2 degeneracy can not be lifted by the SOC and the Mott-Hubbard gap can be attained only when the on-site U is introduced. Thus break-

ing the time-reversal symmetry is essential to get the insulating ground state of Sr_2IrO_4. In the case of Na_2IrO_3, however, the broken time-reversal symmetry is not required to acquire the insulating state. As shown in Fig. 1(b), the SO-split e_{AB} bands are separated over the whole BZ so that the increase of the SOC strength can enlarge the already present gap between two e_{AB} bands. To probe this idea, we carried out DFT calculations by controlling the SOC strength, which can be achieved by changing the scaling factor when generating the j-dependent pseudo-potential[14]. Calculated results for the scale factors $\lambda_{\rm SO}/\lambda_0$= 0.5, 1.0, 1.5, and 2.0 are shown in Fig. 2. Taking the original SOC in the real Ir atom as λ_0 as a reference, $\lambda_{\rm SO}/\lambda_0$= 1.5 was found to be enough to open a full insulating gap. We call these insulating ground states as spin-orbit (SO) insulators, which have energy gaps generated by the SOC. SO insulators have no local moment and preserve the time-reversal symmetry and thus are distinct from the Mott-Hubbard insulator.

To understand the origin of SO insulators, we consider the SOC matrix elements within the e'_g subspace. Since the degenerate e'_g states can be written by

$$
\begin{aligned}
\mid e'_1\rangle &= \frac{1}{\sqrt{3}}(\mid d_{xy}\rangle + e^{\imath\theta} \mid d_{yz}\rangle + e^{-\imath\theta} \mid d_{zx}\rangle) \\
\mid e'_2\rangle &= \frac{1}{\sqrt{3}}(\mid d_{xy}\rangle + e^{-\imath\theta} \mid d_{yz}\rangle + e^{\imath\theta} \mid d_{zx}\rangle) \qquad (1)
\end{aligned}
$$

where $\theta = 2\pi/3$, the on-site SOC term becomes

$$
\langle \mathcal{H}_{\rm SO}\rangle_{e'_g} = \langle \lambda_{\rm SO}\mathbf{L}\cdot\mathbf{S}\rangle_{e'_g} = \frac{\lambda_{\rm SO}}{2}\left(\begin{array}{c|c} \hat{n}\cdot\vec{\sigma} & \\ \hline & -\hat{n}\cdot\vec{\sigma} \end{array}\right) \qquad (2)
$$

where the basis sets are $\mid e'_g\rangle\otimes \mid S=\frac{1}{2}\rangle = \{\mid e'_1\alpha\rangle, \mid e'_1\beta\rangle, \mid e'_2\alpha\rangle, \mid e'_2\beta\rangle\}$ and $\hat{n}$ is the unit vector along the c-axis, i.e., the [111] direction in the local coordinate of IrO_6 octahedron. This block-diagonal form comes from the fact that $\langle\mathbf{L}\rangle$ is simultaneously diagonalized within e'_g manifold and its eigenvalues are $\hat{n}$ and $-\hat{n}$, respectively. Here the SOC terms in e'_g act as an internal magnetic field perpendicular to the ab-plane. The internal field gives rise to an effective Zeeman splitting, but the field direction in the e'_1 component is opposite to that in the e'_2 component. Thus, the effective Zeeman coupling does not break the time-reversal symmetry and $|e'_1\alpha\rangle$–$|e'_2\beta\rangle$ and $|e'_1\beta\rangle$–$|e'_2\alpha\rangle$ remain as time-reversal partners. Since the e_{AB} states are the anti-bonding combination of the e'_g orbitals of neighboring Ir atoms, the splitting of e_{AB} bands by the effective Zeeman coupling is proportional to the SOC strength as shown in Fig. 2, especially at the Γ point.

The ground states of Na_2IrO_3 with the large SOC strength are SO insulators. The band gaps are induced by the effective Zeeman coupling of the SOC within the e'_g subspace. Their characters are different from other types of band insulators such as covalent or ionic ones. The Fermi level is placed between bonding and anti-bonding bands in covalent solids and between different ionic configurations in ionic solids. In SO insulators, the gap is not driven by bonding characters, but mainly related to the symmetry of the states at $E_{\rm F}$. In a sense that their band gaps are generated by the SOC, SO insulators share the same ground with topological insulators though it is necessary to prove the non-trivial topology of its ground state.

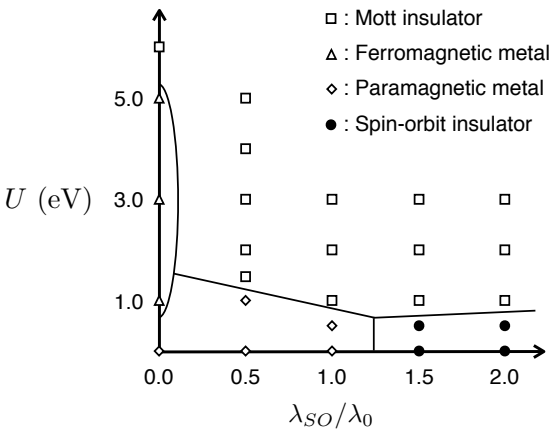

FIG. 3: Phase diagram in the $\lambda_{\rm SO}$–U parameter space depicting four different phases from LDA+U+SO calculations with varying U and $\lambda_{\rm SO}$ values. Paramagnetic metallic phase appears near the origin, Mott insulator in the region of $U > 1$, and SO insulator in the region of $\lambda_{\rm SO} > 1$ and $U < 1$. The real ground state is located inside Mott insulating territory.

One important consequence of the SO insulating phase is the proximity of the AFM ground state to the SO insulator state. In the LDA+U+SO calculation, the AFM ordered local moments are aligned in the ab-plane. Due to the huge internal field along [111] direction, it is hard to break the time-reversal symmetry and to develop local magnetic moments along that direction. Thus, transverse magnetic moments which are perpendicular to the internal field can be easily developed. Strong magnetic anisotropy originated from the internal magnetic fields might be seen in magnetic susceptibility measurements.

To elucidate the relation between SO insulator and AFM Mott insulator phases, we explored a possible phase diagram of Na_2IrO_3 in an extended $\lambda_{\rm SO}$–U parameter space and present the result in Fig. 3. When U is small and $\lambda_{\rm SO}/\lambda_0$ is less than 1.5, the ground state remains as a paramagnetic metal. When there is no SOC, i.e., $\lambda_{\rm SO} = 0$, a ferromagentic metallic phase develops in a narrow range of the parameter space with $\lambda_{\rm SO} = 0$ upto $U = 5.0$ eV. This ferromagnetic state becomes unstable in the presence of the SOC. On the other hand, for the value of U smaller than about 1 eV, the SO insulator phase emerges as a non-magnetic insulator. Since the band gap is induced by the effective Zeeman coupling of the SOC within the e'_g subspace, the Kramers degeneracy of the valence states holds up and the time-reversal symmetry remains unbroken. For the finite $\lambda_{\rm SO}$, Mott insulating AFM states develop as U becomes larger than about 1.0 eV. The difference between two insulating phases, i.e., the criterion for the boundary is the existence of local magnetic moments. The Mott insulating phase has AFM ordering where on-site Coulomb repulsion breaks the symmetry developing local moments during the correlation gap opens. Our LDA+U+SO calculation predicts that the real ground state of Na_2IrO_3 is

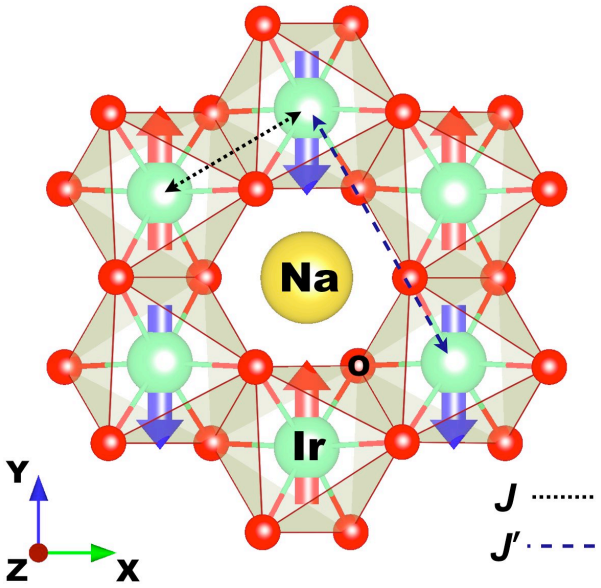

FIG. 4: (Color online) Schematic drawing of the $(Ir_{2/3}Na_{1/3})O_2$ plane and magnetic configuration of the AFM insulating ground state of Na_2IrO_3. Magnetic moments are ordered anti-ferromagnetically lying on the ab-plane due to the strong internal field along the c-axis. Not only the NN exchange J (dotted arrow) but the NNN exchange J' (dashed arrow) are significant and may give rise to magnetic frustration.

located in the Mott AFM region with $U = 2.0 \sim 3.0$ eV and $\lambda_{SO}/\lambda_0 = 1$. However, the strongly anisotropic nature of its AFM ordering originates from its proximity to the SO insulator phase.

Another important aspect in Na_2IrO_3 is magnetic frustration indicated in large θ_{CW}/T_N ratio from susceptibility measurements[13]. To reveal the origin of frustration, we have estimated exchange interactions J and J' between nearest-neighbor (NN) and next-nearest-neighbor (NNN) Ir atoms respectively.(Fig. 4) Calculation scheme is based on the perturbation formalism.

$$J_{ij} = \frac{1}{2\pi}\int^{\epsilon_F} d\epsilon \left[\hat{G}^{\uparrow}_{ij}\hat{V}_j\hat{G}^{\downarrow}_{ji}\hat{V}_i\right], \qquad (3)$$

where $\hat{G}$ is the one-particle Green's function and $\hat{V}$ is on-site exchange interaction potential[20]. The result is $J'/J = 0.47$, which means that NN and NNN exchange coupling strength are comparable and they might be a source of frustration. Above result is mainly attributed to the extended nature of Ir $5d$ orbitals. Large direct overlap between NN Ir atoms gives FM direct exchange interaction, competing with AFM superexchange from oxygen mediated hopping channels and finally reducing AFM exchange J. On the other hand, the NNN hopping integrals are not negligible that the NNN AFM interaction J' can be comparable and frustrate long range AFM ordering.

In conclusion we have shown that the spin-orbit entangled e'_g states under the strong internal Zeeman field driven by the SOC lead to an unusual band gap. The predicted AFM ground state is in close proximity to the SO insulator phase where the AFM ordering in Na_2IrO_3 becomes strongly anisotropic with quenched moments along the c-axis. The highly anisotropic AFM state in Na_2IrO_3 may serve as a model system for the two-dimensional XY model with frustrated exchange interactions. One may be able to drive a crossover between AFM and SO insulators through the modulation of structural parameters or chemical substitution, though we need more study on the role of SOC in the Mott AFM phase in connection with the topological nature of SO insulators.

Acknowledgments

We are grateful to H. Takagi for sharing information prior to publication. This work was supported by the KOSEF through the ARP (R17-2008-033-01000-0). We also acknowledge the support from KISTI under the Supercomputing Application Support Program.

* Corresponding author. Electronic address:jyu@snu.ac.kr

[1] T. Kimura, T. Goto, H. Shintani, K. Ishizaka, T. Arima, and Y. Tokura, Nature **426**, 55 (2003).
[2] N. Hur, S. Park, P. A. Sharma, J. S. Ahn, S. Guha, and S.-W. Cheong, Nature **429**, 392 (2004).
[3] R. Karplus and J. M. Luttinger, Phys. Rev. **95**, 1154 (1954).
[4] S. Murakami, N. Nagaosa, and S.-C. Zhang, Science **301**, 1348 (2003).
[5] J. Sinova, D. Culcer, Q. Niu, N. A. Sinitsyn, T. Jungwirth, and A. H. MacDonald, Phys. Rev. Lett. **92**, 126603 (2004).
[6] H. Zhang, C.-X. Liu, X.-L. Qi, X. Dai, Z. Fang, and S.-C. Zhang, Nature Physics **5**, 438 (2009).
[7] Y. Xia, D. Qian, D. Hsieh, L. Wray, A. Pal, H. Lin, A. Bansil, D. Grauer, Y. S. Hor, R. J. Cava, et al., Nature Physics **5**, 398 (2009).
[8] C. L. Kane and E. J. Mele, Phys. Rev. Lett. **95**, 146802 (2005).
[9] B. J. Kim, H. Jin, S. J. Moon, J.-Y. Kim, B.-G. Park, C. S. Leem, J. Yu, T. W. Noh, C. Kim, S.-J. Oh, et al., Phys. Rev. Lett. **101**, 076402 (2008).
[10] S. J. Moon, H. Jin, K. W. Kim, W. S. Choi, Y. S. Lee, J. Yu, G. Cao, A. Sumi, H. Funakubo, C. Bernhard, et al., Phys. Rev. Lett. **101**, 226402 (2008).
[11] A. Shitade, H. Katsura, J. Kuneš, X.-L. Qi, S.-C. Zhang, and N. Nagaosa, Phys. Rev. Lett. **102**, 256403 (2009).
[12] C. L. Kane and E. J. Mele, Phys. Rev. Lett. **95**, 226801 (2005).
[13] H. Takagi, (private communications).
[14] The DFT code, OpenMX, is available at the web site (http://www.openmx-square.org) in the constitution of the GNU

General Public License.
[15] T. Ozaki, Phys. Rev. B **67**, 155108 (2003).
[16] M. J. Han, T. Ozaki, and J. Yu, Phys. Rev. B **73**, 045110 (2006).
[17] K. M. Mogare, K. Friese, W. Klein, and M. Jansen, Z. Anorg. Allg. Chem. **630**, 547 (2004).
[18] Choong H. Kim, et al., (unpublished).
[19] L. F. Mattheiss, Phys. Rev. B **13**, 2433 (1976).
[20] M. J. Han, T. Ozaki, and J. Yu, Phys. Rev. B **70**, 184421 (2004).